

Numerical modelling of a continuous wave Yb:doped bulk crystal laser emitting on a three-level laser transition around 980 nm

Sylvie Yiou, François Balembois, Patrick Georges

▶ **To cite this version:**

Sylvie Yiou, François Balembois, Patrick Georges. Numerical modelling of a continuous wave Yb:doped bulk crystal laser emitting on a three-level laser transition around 980 nm. Journal of the Optical Society of America B, 2005, 22 (3), pp.572-581. hal-00686983

HAL Id: hal-00686983

https://hal-iogs.archives-ouvertes.fr/hal-00686983

Submitted on 11 Apr 2012

HAL is a multi-disciplinary open access archive for the deposit and dissemination of scientific research documents, whether they are published or not. The documents may come from teaching and research institutions in France or abroad, or from public or private research centers.

L'archive ouverte pluridisciplinaire **HAL**, est destinée au dépôt et à la diffusion de documents scientifiques de niveau recherche, publiés ou non, émanant des établissements d'enseignement et de recherche français ou étrangers, des laboratoires publics ou privés.

Numerical modeling of a continuous-wave Yb-doped bulk crystal laser emitting on a three-level laser transition near 980 nm

Sylvie Yiou, François Balembois, and Patrick Georges

Laboratoire Charles Fabry de l'Institut d'Optique, Unité Mixte de Recherche 8501 du Centre National de la Recherche Scientifique, Centre Universitaire Paris XI, Bât. 503, 91403 Orsay, France

Received February 2, 2004; revised manuscript received September 17, 2004; accepted October 5, 2004

We present a new model for cw, Yb-doped, bulk crystal lasers emitting on a three-level laser transition near 980 nm. This model takes into account the saturation of the absorption and the spatial evolution of the pump and laser beams inside the crystal, which are two important points in three-level lasers. We have validated our numerical model by building an efficient cw Yb:S-FAP (ytterbium:strontium-fluoroapatite) laser emitting at 985 nm and pumped at 899 nm by a Ti:sapphire laser. Our model can be used to define the parameters that optimize the laser output power at 985 nm, such as the relative sizes of the pump and laser beams, the optimum output coupler, or characteristics of the crystal (length, Yb concentration). By adapting this model to diode pumping, we have established the conditions to obtain cw, efficient laser operation at 985 nm of an Yb:S-FAP crystal pumped by a standard $1 \times 100\text{-}\mu m^2$ laser diode. © 2005 Optical Society of America

OCIS code: 140.3580.

1. INTRODUCTION

Examples of three-level lasers are not widespread in the literature. The main three-level systems that are reported to produce a laser effect are the Cr^{3+} ion in the ruby laser[1] and the Er^{3+} and Yb^{3+} ions, mainly in silica fibers.[2,3] Three-level lasers have also been realized with Mn^{5+} ions in a barium vanadate crystal[4] and Tm^{3+} ions in a YAG crystal[5] but remain marginal. These few examples illustrate the difficulty of obtaining a laser effect on a three-level laser transition. Indeed the major drawback of three-level lasers is that the lower laser level is the ground-state level. The result is that the material is not transparent at the laser wavelength without pumping. As a consequence a high pump density is necessary to invert half the total population to reach transparency. Moreover, a good overlap between the pump and the laser beams in the active medium is needed to avoid absorption at laser wavelength by the unpumped zones. Both conditions can be achieved in fiber lasers because of the small size of the fiber core. Broad-area diode pumping of fiber lasers emitting near 980 nm was indeed initially reported by Minelly *et al.*[6] More recently a cw output power of 3.5 W at 977 nm has been obtained by Ylä-Jarkko *et al.* with a special Yb-doped fiber pumped by two laser diodes.[7]

Despite the remarkable performance of Yb-doped fiber lasers, the use of Yb-doped bulk crystals remains interesting because of the prospect of realizing compact systems without the need for special fiber technologies. It would also be of interest to benefit from the recent progress in the growth of high-optical-quality, Yb-doped crystals.[8] However, in bulk crystals the strong divergence of the pump-diode beam obviates a good overlap between the pump and the laser beams. The spatial evolution of the beams is also very important in bulk crystals, which is not the case in fiber lasers. The only three-level, Yb-doped crystal lasers at 985 nm reported in the literature are a long-pulse-pumping, quasi-cw, ytterbium:strontium-fluoroapatite (Yb:S-FAP) laser[9] and a Ti:sapphire-pumped, cw, Yb:C_4SFAP laser with a low slope efficiency (5%) and a high laser threshold (516 mW).[10] This illustrates the difficulty of obtaining a laser effect on a three-level laser transition in bulk crystals.

In this work we present a numerical model for cw, Yb-doped, bulk crystal lasers emitting on the three-level laser transition near 980 nm that is not usually studied in these crystals. Our goal is to have a better understanding of the laser behavior and then to show guidelines useful for building efficient, three-level, Yb-doped, bulk crystal lasers with a low laser threshold.

The numerical model that we have developed is specific to cw, three-level, Yb-like-doped, bulk crystal lasers because there is a lack of such a model in the literature. Three-level laser transitions such as the transitions in Er^{3+} at 1.5 μm and in Yb^{3+} at 980 nm are well known in fibers. Theoretical models for Er^{3+} and Yb^{3+}-doped fiber amplifiers and lasers near these wavelengths have already been proposed.[2,3,11,12] However, these models are not suited to bulk crystals because the spatial evolution of the beam sizes along the propagation axis is not taken into account, which is very important in our case.

The transition near 1050 nm usually studied in Yb-doped materials is a quasi-three-level transition, i.e., the lower laser level is located in the ground-state manifold and has an energy of a few hundreds of reciprocal centimeters depending on the material. In the literature several models of a quasi-three-level transition in an end-pumped, cw, bulk crystal laser have been reported. The models from Risk[13] and Fan and Byer[14] have the advan-

tage of considering the overlap between the pump and laser beams. However, they neglect the depletion of the lower laser level and so are not available for three-level lasers. The models from Bourdet[15] and Lim and Izawa[16] do not make this latter approximation but consider that the pump and laser beams are uniform in the transverse dimension, so the overlap between the pump and laser beams is not taken into account. The model from Augé *et al.*[17] does not make these two approximations and include the effect of saturation of the absorption. Nevertheless, in this model saturation of the absorption is accounted for with experimental measurements of the absorption. This means experiments are needed in advance to compute the performance of the laser.

Compared with the latter model, our model includes calculation of saturation of the absorption with only the spectroscopic data for the crystal that can be found in the literature. Hence the originality of our model specific to cw, three-level, bulk crystal lasers is to account for the spatial evolution of the pump and laser beams in the crystal and for saturation of the absorption without the approximations made by Augé *et al.*[17] mentioned above. This model has been experimentally validated by building an Yb:$Sr_5(PO_4)_3F$ (or Yb:S-FAP) crystal laser emitting at 985 nm. This model can then be applied to predict the laser threshold and performance of any cw, pumped, Yb-like-doped bulk crystal on a three-level transition. Such Yb-doped crystal lasers emitting near 980 nm are interesting for the pumping of Er-doped fiber amplifiers. Moreover, these lasers could be used to achieve the blue range by second-harmonic generation.

In Section 2 we describe our model. In Section 3 we compare the results of the numerical simulations with the experimental results obtained at 985 nm with an Yb:S-FAP crystal pumped with a cw Ti:sapphire laser. In Section 4 we discuss the parameters to optimize the laser performance near 980 nm. In Section 5 we adapt the model to diode pumping and present the corresponding optimized parameters.

2. THEORY

The first goal of our model is to determine if it is possible to reach laser threshold on the three-level laser transition of an Yb-doped bulk crystal with small cw pump power, i.e., a few hundreds of milliwatts. We first present the equations of the model (Subsection 2.A) and then calculate the gain at threshold (Subsection 2.B). The second goal is to estimate the cw output power at 985 nm versus the incident pump power (Subsection 2.C).

A. Equations of the Model

As an example Fig. 1 represents the energy levels implied in an Yb:S-FAP crystal.[18] In this three-level laser system the lower laser level is the ground-state level that is strongly populated. The temperature has only a small effect on the population of this level; it is almost not temperature populated, so we did not consider any thermal dependence. σ_{ap} and σ_{ep} are the effective absorption and emission cross sections at pump wavelength λ_p, respectively. σ_{al} and σ_{el} are, respectively, the effective absorption and emission cross sections at laser wavelength λ.[19]

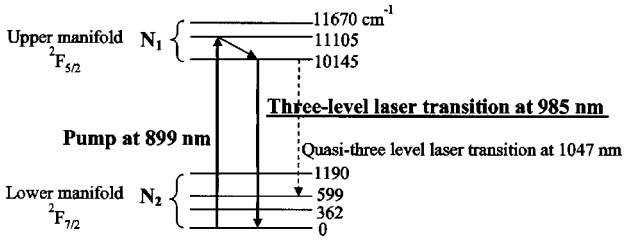


Fig. 1. Energy diagram of Yb in S-FAP host showing the pump and three-level laser transitions and the notations used in the model. The quasi-three-level transition that is usually studied is in dashed line.

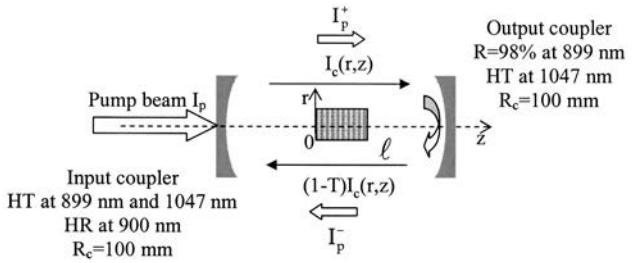


Fig. 2. Laser cavity and notations.

τ is the fluorescence lifetime. N_1 and N_2 are, respectively, the population densities of the lower and upper manifolds. N is the total doping-ion (Yb) concentration.

$$N = N_1 + N_2. \tag{1}$$

The z axis is the optical axis with its origin at the entrance of the crystal. In Sections 2, 3, and 4 we assume that the pump beam and the cavity beam present a symmetry of revolution about the z axis. We assume that all functions can be described in cylindrical coordinates (r, z). The pumping is longitudinal. The radial coordinate r is perpendicular to the z axis (see Fig. 2). We assume that the cavity laser beam is TEM_{00}. I_p and I are the pump and laser intensities, respectively (in W/cm^2). In the following the resolution of I_p is one of the keys of our numerical model.

We assume that the cavity beam has a Gaussian profile and that the laser power in the cavity is independent of z (which is justified for low cavity losses). Neglecting spatial hole-burning, the laser intensity I is

$$I(r, z) = (2 - T)I_c(r, z), \tag{2}$$

with

$$I_c(r, z) = \frac{2P_{out}}{T\pi\omega_c^2(z)} \exp\left[-\frac{2r^2}{\omega_c^2(z)}\right]. \tag{3}$$

T is the transmission of the output coupler and P_{out} is the laser output power (see Fig. 2). $\omega_c(z)$ is the radius of the cavity beam at the abscissa z in the crystal at $1/e^2$ of the maximum intensity.

$$\omega_c(z) = \omega_{c_0}\left\{1 + \left[\frac{\lambda}{\pi n \omega_{c_0}^2}(z - z_{c_0})\right]^2\right\}^{1/2}. \tag{4}$$

n is the index of refraction of the crystal, ω_{c_0} is the waist of the cavity beam inside the crystal, and z_{c_0} is the ab-

scissa of the waist in the crystal. In the case described here $z_{c_0} = \ell/2$, where ℓ is the crystal length.

The equations leading to the expression of the gain coefficient g at laser wavelength can be found in Ref. 17. Let us recall that

$$g = \sigma_{el} N_2 - \sigma_{al} N_1 . \tag{5}$$

The rate equations for N_1 and N_2 give the expression for g (where σ_{ep} has been neglected):

$$g = N \frac{\sigma_{el}\sigma_{ap}\frac{\lambda_p}{hc} I_p - \frac{\sigma_{al}}{\tau}}{\sigma_{ap}\frac{\lambda_p}{hc} I_p + (\sigma_{el} + \sigma_{al})\frac{\lambda}{hc} I + \frac{1}{\tau}} . \tag{6}$$

This equation gives the expression of the pump intensity I_{tr} necessary to reach transparency near 980 nm obtained when g is equal to zero:

$$I_{tr} = \frac{hc}{\lambda_p} \frac{\sigma_{al}}{\sigma_{el}\sigma_{ap}} \frac{1}{\tau} . \tag{7}$$

With the low-loss approximation the final expression of the gain G per double pass integrated over the whole crystal can be written as

$$G = \left[1 + \int_0^{\ell} dz \int_0^{r_c} \frac{4g(r, z)}{\omega_c^2(z)} \exp\left(-\frac{2r^2}{\omega_c^2(z)} \right) r\, dr \right]^2 . \tag{8}$$

r_c is the crystal radius (to simplify, we assume that the crystal has a right circular cylindrical section). This formula is also correct for crystals with a square section if its size is much larger than the beam dimensions. The low-loss approximation remains valid for gain G as high as ≈ 2; at this value this approximation introduces a relative error of approximately 13% of the gain, which is still tolerable. That is why we have limited our calculations to the value $G = 2$.

At laser threshold, the gain is equal to the losses:

$$G = \frac{1}{(1 - T)(1 - L)} , \tag{9}$$

where L represents the passive losses in the cavity. L is the only adjustable parameter of our model. For a given pump power Eq. (9) has to be solved numerically to find the value of the output power.

B. Gain at Laser Threshold ($I = 0$)

To solve Eq. (9), the combining of Eqs. (6) and (8) shows that it is necessary to know the evolution of the pump intensity in the crystal $I_p(r, z)$. For that we have to account for the saturation of the absorption. The differential equation that gives the pump intensity $I_p(r, z)$ is

$$\frac{dI_p}{dz} = -\alpha_p I_p , \tag{10}$$

with

$$\alpha_p = \sigma_{ap} N_1 - \sigma_{ep} N_2 . \tag{11}$$

α_p is the absorption coefficient at pump wavelength.

Finally, the evolution of the pump intensity in the crystal is given by

$$\frac{dI_p}{dz} = -N \frac{\sigma_{ap}\sigma_{el} I + \sigma_{ap}/\tau}{\sigma_{ap} I_p + (\sigma_{el} + \sigma_{al}) I + 1/\tau} I_p . \tag{12}$$

In this formula we have neglected σ_{ep}, which is justified with regard to the emission spectrum given in Ref. 18. In their model, Augé *et al.* have kept the classical form of a decreasing exponential for $I_p(r, z)$, and the absorption coefficient α_p was introduced experimentally.[17] In our work we have studied numerically the evolution of the pump profile with knowledge only of the spectroscopic data, a factor in the originality of our model.

We assume that the transverse pump profile is Gaussian and write

$$I_p(r, z) = I_{p_0}(z) \exp\left(-\frac{2r^2}{\omega_p^2(z)} \right) . \tag{13}$$

$I_{p_0}(z)$ is the pump intensity along the propagation axis ($r = 0$). $\omega_p(z)$ is the radius of the pump beam at the abscissa z in the crystal at $1/e^2$ of the maximum intensity, and is given by

$$\omega_p(z) = \omega_{p_0} \left\{ 1 + \left[M_p^2 \frac{\lambda}{\pi n \omega_{p_0}^2} (z - z_{p_0}) \right]^2 \right\}^{1/2} . \tag{14}$$

n is the index of refraction of the crystal, ω_{p_0} is the waist of the pump beam inside the crystal, and z_{p_0} is the abscissa of the waist in the crystal. In the following $z_{p_0} = \ell/2$, corresponding to the experiment. M_p^2 is the quality factor of the pump beam and is assumed to be equal to 1 in this Subsection 2.B since the laser pump is a TEM_{00} laser.

First we study the saturation of the absorption without laser effect [$I = 0$ in Eq. (12)] to determine the gain G at laser threshold. The first step is to calculate the pump intensity $I_{p_0}(z)$ along the propagation axis ($r = 0$). In these conditions the equation satisfied by $I_{p_0}(z)$ is

$$\frac{dI_{p_0}}{dz} = \frac{-\alpha_{p_0}}{1 + (I_{p_0}/I_{p_{sat}})} I_{p_0} . \tag{15}$$

$\alpha_{p_0} = \sigma_{ap} N$ is the nonsaturated absorption coefficient and $I_{p_{sat}} = (hc/\lambda_p)(1/\sigma_{ap}\tau)$ is the saturation pump intensity. In the general case Eq. (15) gives an implicit expression of I_{p_0} as a function of the abscissa z. To determine I_{p_0} we have decomposed the crystal along the z axis into 100 slices, the size of each slice being $dz = \ell/100$. This size was small enough to validate the assumption that the pump intensity was constant in each slice. At $z = 0$ the pump intensity is

$$I_{p_0}(0) = \frac{hc}{\lambda_p} \frac{2P_{in}}{\pi \omega_p^2(0)} . \tag{16}$$

P_{in} is the incident pump power (in watts). The fraction of pump power that is absorbed in the crystal is $1 - I_{p_0}(\ell)/I_{p_0}(0)$. To show the importance of saturation

of the absorption we have reported the absorption of the pump power in the crystal depicted in Table 1 (which corresponds to the crystal used in our experiments) with and without saturation versus the incident pump power in Fig. 3. This plot shows that the fraction of absorbed pump power in the crystal used in our experiments decreases when the pump power increases and saturates at the value of 10% for the maximum available pump power of 1.5 W.

In a second step we studied the transverse profile of the pump intensity to verify that the pump profile remained Gaussian during the propagation along the crystal. The principle of the calculation is the same as that described above: For each slice of size $\ell/100$ we have decomposed the crystal into 100 crowns of $r_c/100$ radius. At $z = 0$ we assume that the pump profile is Gaussian and write

$$I_p(r, 0) = I_{p_0}(0)\exp[-2r^2/\omega_p^2(0)]. \tag{17}$$

For $0 \leqslant i \leqslant 100$ and for $0 \leqslant j \leqslant 100$ we can calculate $I_p(i\, r_c/100, j\, \ell/100)$, thanks to Eq. (12) (with $I = 0$). The result of the numerical simulations is that the transverse profile of the pump intensity remains Gaussian during the propagation in the crystal used in our experiments, so the expression of $I_p(r, z)$ given in Eq. (13) is justified.

We have seen that the fraction of absorbed pump power in our crystal is low (about 10%), so we wanted to use the available pump power more efficiently by means of a double pass of the pump beam in the crystal by reflection in the output mirror (see Fig. 2). The expression of the pump intensity is then modified. Let us establish its expression along the z axis without laser effect. Neglecting interference effects we can write $I_{p_0}(z)$ as

$$I_{p_0}(z) = I_{p_0}^+(z) + I_{p_0}^-(z). \tag{18}$$

$I_{p_0}^+(z)$ refers to the pump wave that propagates in the direction of increasing z, whereas $I_{p_0}^-(z)$ refers to the pump wave that propagates in the opposite direction. $I_{p_0}^+(z)$ and $I_{p_0}^-(z)$ both satisfy Eq. (12), and with the approach followed by Rigrod[20] we find that for any z

$$I_{p_0}^+ I_{p_0}^- = K_p. \tag{19}$$

K_p is a constant that does not depend on the spatial variables r and z, but on the incident pump power. To find K_p we used the limit condition $I_{p_0}^-(\ell) = R I_{p_0}^+(\ell)$. R is the reflection coefficient of the output mirror at the pump wavelength ($R = 98\%$ under the experimental conditions). Then we have $K_p = R[I_{p_0}^+(\ell)]^2$. We can deduce $I_{p_0}^+(\ell)$ from Eq. (12) (with $I = 0$) by replacing I_p by $I_{p_0}^+$, yielding

Table 1. Parameters of the Yb:S-FAP Crystal Used in the Experiment and in Sections 2 and 3 and Subsections 4.A and 4.B

Refractive Index (at 985 nm)	Length	Radius	Yb Concentration
1.62[a]	0.43 cm	0.2 cm	1.9×10^{19} ions/cm^3

[a] For $E \| c$ and $E \perp c$ at this precision.

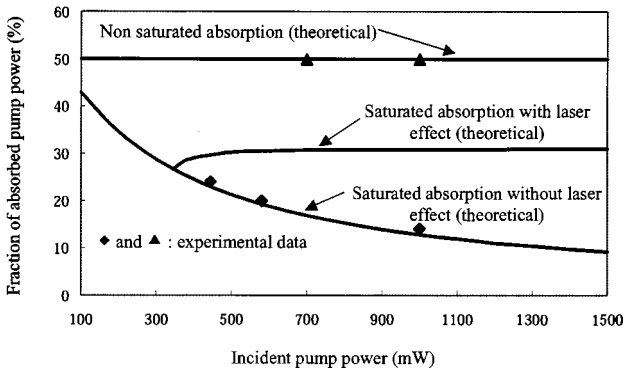


Fig. 3. Theoretical absorption of the pump in the crystal (described in Table 1) versus incident pump power in the nonsaturated regime, in the saturated regime without laser effect, and in the saturated regime with laser effect. Comparison is shown with the experimental data obtained in the nonsaturated regime and in the saturated regime without laser effect.

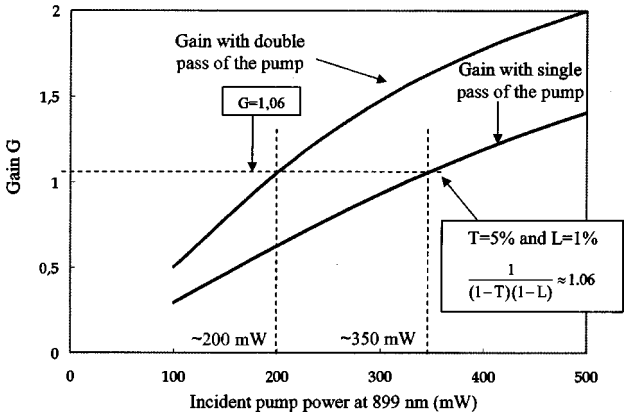


Fig. 4. Gain G versus incident pump power for a single pass and a double pass of the pump in the crystal (described in Table 1).

$$I_{p_0} = I_{p_0}^+ + \frac{K_p}{I_{p_0}^+}. \tag{20}$$

Once the passive losses L and the transmission of the output coupler T are fixed, it is possible to deduce the pump power necessary to reach laser threshold by calculation of the gain G with Eq. (8). Figure 4 shows gain G versus incident pump power for a single pass and for a double pass of the pump in the crystal. For a double pass the pump waist locations on the two passes are assumed to be at the same location, i.e., in the middle of the crystal. In the example shown in Fig. 4 the pump waist ω_{p_0} is 80 μm and the cavity waist ω_{c_0} is 40 μm. This plot shows that for typical passive losses L of 1% and for a transmission of the output coupler T of 5% corresponding to a gain G of about 1.06, it is possible to reach laser threshold with a cw incident pump power of ≈350 mW with a single pass of the pump. The incident pump power at laser threshold is only 200 mW with a double pass of the pump.

C. Study of the cw Output Power at 985 nm ($I \neq 0$)

With laser effect the problem is more complicated, since the pump profile along the z axis also depends on the laser intensity in the cavity as evidenced by Eq. (12). The

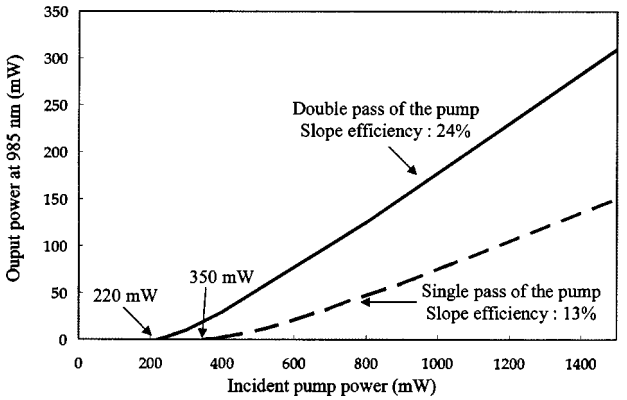


Fig. 5. Example of theoretical output power at 985 nm versus incident pump power for a single pass and a double pass of the pump in the crystal.

stimulated emission brings the excited ions back to the fundamental level which again generates absorption at the laser wavelength. As a consequence it is more difficult to saturate the absorption at pump wavelength with laser effect. So the absorption of the pump with laser effect is intermediate between nonsaturated absorption and saturated absorption without laser effect. This is illustrated in Fig. 3 where we have plotted the fraction of absorbed pump power in these three different processes versus incident pump power.

Once the gain G_{th} at laser threshold is calculated, it is possible to determinate the laser output power at 985 nm by increasing the incident pump power and computing the gain G with $I \neq 0$. We make I, i.e., P_{out}, vary. The value of P_{out} for which G is equal to G_{th} is the output power. Figure 5 shows an example of laser efficiency curves, i.e., output power at 985 nm versus incident pump power with a single pass and a double pass of the pump in the crystal. This plot shows that the double pass of the pump enables one to increase the slope efficiency by almost a factor of 2.

3. COMPARISON BETWEEN THE MODEL AND THE EXPERIMENTAL RESULTS

The experimental setup is described in Fig. 2. We used a double pass of the pump by reflection in the output mirror at pump wavelength. The crystal used for this experiment was an Yb:S-FAP crystal chosen from a list of Yb-doped crystals with a criterion that it exhibit the lowest pump intensity necessary to reach transparency (see Table 2). The parameters of the crystal that we used are reported in Table 1. The crystal of Yb:S-FAP was longitudinally pumped by a cw, Ti:sapphire laser emitting a maximum output power of 1.45 W in a diffraction-limited beam at 899 nm, corresponding to the maximum of absorption of the Yb:S-FAP crystal. The waist of the pump beam inside the rod was 80 μm. We measured the saturated absorption of the pump in the crystal. The experimental data are reported in Fig. 3 and are in good agreement with the theory. The absorption of the pump in the crystal was only 14% for an incident pump power of 1 W, showing that our crystal was not optimized. The corresponding nonsaturated absorption of the pump was 50%. The laser cavity was nearly concentric with a radius of curvature of the concave mirrors of 100 mm. The waist of the laser beam inside the rod was measured to be approximately 40 μm. These conditions correspond closely to the optimal conditions determined by the model. Figure 6 shows the experimental laser output power at 985 nm versus incident pump power obtained with output couplers of 7% and 22% as well as a comparison with the plots resulting from our numerical model. In both cases the adjustable parameter L is 2.5%. These passive losses L are mostly attributed to diffusion in the Yb:S-FAP crystal. Experimental and theoretical data are in good agreement. Best performance was obtained with the output coupler of 7%. The Yb:S-FAP laser has delivered a cw output power of 250 mW at 985 nm for an incident pump power of 1.45 W.

We also made gain measurements by introducing known losses into the cavity and finding the laser thresh-

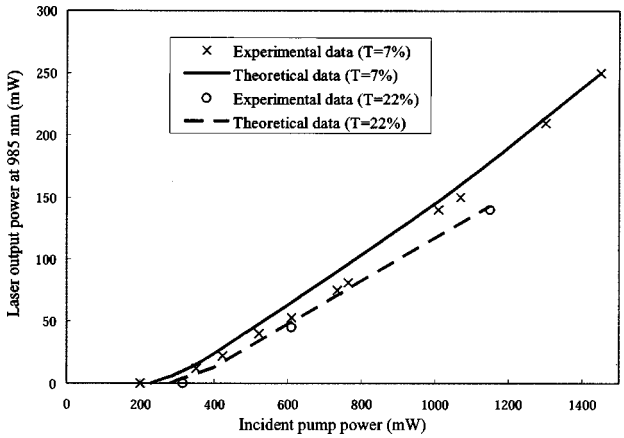


Fig. 6. Experimental laser output power at 985 nm versus incident pump power for two different output couplers $T = 7\%$ and $T = 22\%$; comparison is shown with the model. In both cases the passive losses L are adjusted at 2.5%.

Table 2. Estimation of the Transparency Pump Intensity I_{tr} for Different Yb-Doped Materials

Host Material	λ_p (nm)	λ (nm)	σ_{al} (10^{-20} cm^2)	σ_{ap} (10^{-20} cm^2)	σ_{el} (10^{-20} cm^2)	τ (ms)	I_{tr} (kW/cm^2)
GdCOB[17]	900	976	1.2	0.5	0.5	2.74	38
$LiYO_2$[21]	908	972	0.8	1.2	0.5	1.13	26
YAG[22]	941	968	0.75	0.77	1	0.95	22
Tungstate (KGW)[23]	935 ($E\|a$)	981 ($E\|a$)	12	2.5	16	0.6	10
Apatite (S-FAP)[18]	900 ($E\|c$)	985 ($E\perp c$)	10	9	10	1.14	2

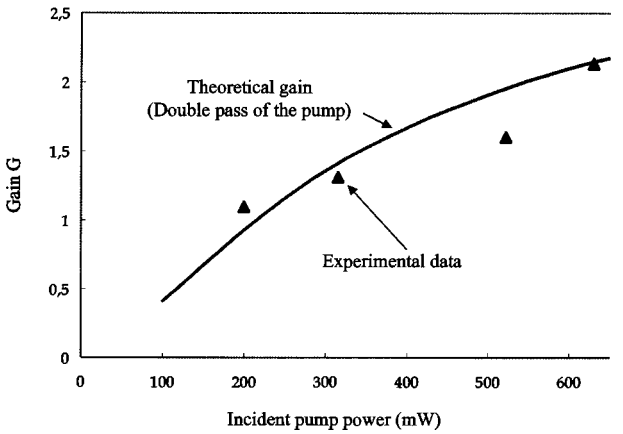


Fig. 7. Experimental gain at laser threshold versus incident pump power (triangles) and comparison with the model (solid curve).

old. The gain at threshold G is indeed equal to $1/[(1 - T)(1 - L)]$, where T represents an equivalent output coupler. The gain at threshold versus incident pump power is reported in Fig. 7. The passive losses L are again adjusted to 2.5%. We have reached an experimental gain of ≈ 2, which is high for an Yb-doped bulk crystal laser. The experimental data are once again in good agreement with the model.

These experiments have enabled us to validate our numerical model for a Yb-doped bulk crystal emitting on a three-level laser transition near 980 nm. Therefore, we have used this model to determine the parameters such as the pump and cavity beam radii, the output coupler, or characteristics of the crystal (length and Yb concentration) that could optimize the cw output power at 985 nm.

4. OPTIMIZATION OF THE LASER OUTPUT POWER AT 985 nm

One of the interests of our numerical model is to predict the performance of a cw, Yb-doped, bulk crystal laser emitting on a three-level laser transition. This model also indicates ways to optimize laser performance by varying different parameters that were fixed until now. These parameters, as just mentioned, are the pump and laser beam waists in the crystal, the transmission of the output coupler, and characteristics of the crystal (length and Yb concentration).

A. Influence of the Relative Beam Sizes in the Crystal

The relative pump and laser beam sizes in the crystal are very important since the cavity beam has to be smaller than the pump beam to prevent absorption at laser wavelength by the unpumped zones. Figure 8 shows laser output power at 985 nm versus cavity waist for a double pass of the pump and for different crystal lengths at an incident pump power of 1.5 W. In this example the transmission of the output coupler is 5%. The passive losses are chosen equal to 1%, which is supposed to be achieved with the recent progress in the growth of Yb:S-FAP crystals. For a given pump waist of 80 μm (corresponding to the experimental conditions), this simulation shows that there is an optimal cavity waist varying between 40 μm and 60 μm according to the crystal length. This situation is different from four-level lasers, where the maximum output power is achieved when the pump and cavity beam sizes are almost equal.[24] Figure 8 shows that when the pump and cavity waists are equal (to 80 μm) the laser output power is, for example, divided by 1.4 when the crystal length is 0.43 cm, meaning that the absorption of the pump is not efficiently saturated at every point in the crystal.

B. Search for the Optimal Output Coupler

The optimal transmission of the output coupler can be evaluated with our model. Figure 9 shows output power at 985 nm versus transmission of the output coupler for different incident pump powers and for a double pass of the pump. The passive losses are 1%. This plot shows that the optimal transmission of the output power is between 5% and 8%, corresponding to that of our experimental output coupler of 7%.

C. Influence of the Crystal Parameters

We have studied the influence of the crystal length and the Yb concentration of the crystal. Figure 10 shows out-

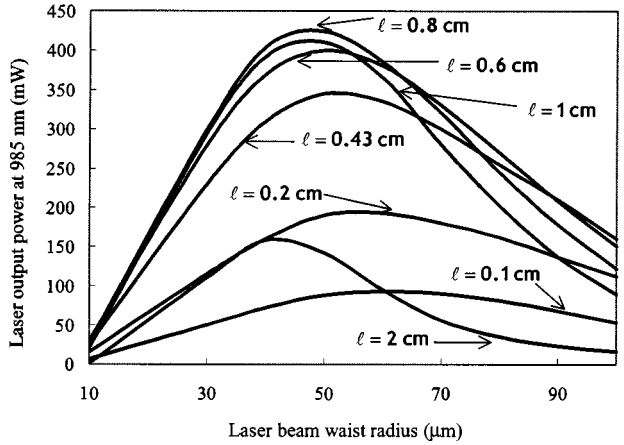


Fig. 8. Search for the optimum size of the laser beam inside the crystal with a double pass of the pump for different crystal length ℓ. Pump beam waist radius is 80 μm, doping level is 1.9×10^{19} ions/cm^3, incident pump power is 1.5 W, transmission of the output coupler is 5%, and passive losses are 1%.

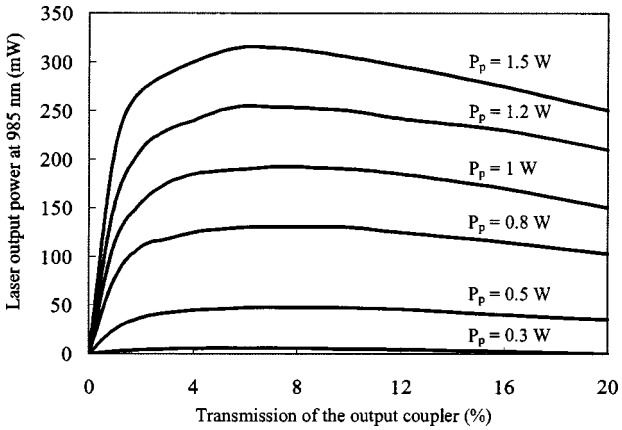


Fig. 9. Search for the optimum output coupler for different values of incident pump power P_p. The crystal used for the simulation is described in Table 1. The passive losses L are 1%.

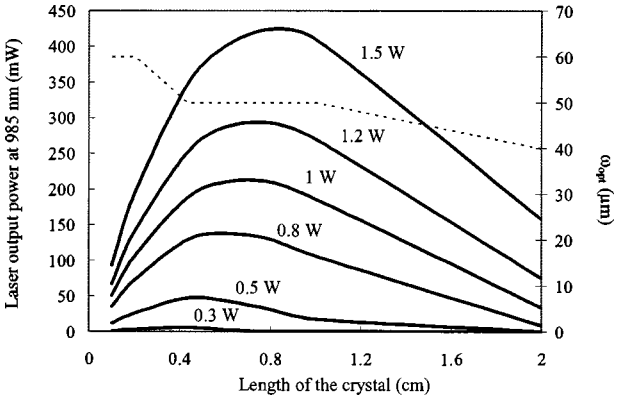


Fig. 10. Output power at 985 nm versus crystal length with a double pass of the pump for different pump powers P_p (left axis). Optimum laser beam waist ω_{opt} was determined by Fig. 8 at the maximum available pump power of 1.5 W versus crystal length (right axis). For each crystal length the output power is calculated with ω_{opt}. Yb concentration N is 1.9×10^{19} ions/cm^3, pump beam waist radius is 80 μm, transmission of the output coupler is 5%, and passive losses are 1%.

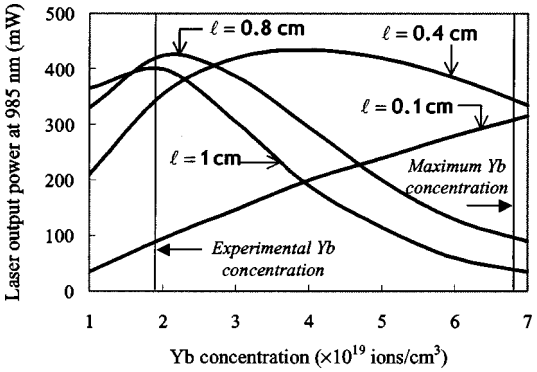


Fig. 11. Influence of the Yb concentration on the output power with a double pass of the pump for different crystal length ℓ. Incident pump power is 1.5 W, laser beam waist radius is 50 μm, pump beam waist radius is 80 μm, passive losses are 1%, and transmission of the output coupler is 5%.

put power at 985 nm versus crystal length with a double pass of the pump for different pump powers P_p, as well as the optimum laser beam waist ω_{opt} determined by Fig. 8 at the maximum available pump power of 1.5 W versus crystal length. For each value of crystal length the output power is calculated with ω_{opt}. The pump beam waist radius is 80 μm. The transmission of the output coupler is 5% and the passive losses are 1%. The Yb concentration N is 1.9×10^{19} ions/cm^3. At this doping level the optimal length of the crystal is approximately 0.8 cm. The absorption of the pump in the crystal is then about 75%.

As for the influence of Yb concentration, Fig. 11 shows the output power at 985 nm versus the Yb concentration for different crystal lengths (maximum pump power of 1.5 W, double pass of the pump, transmission of the output coupler of 5%, passive losses of 1%). The laser beam waist radius is 50 μm and the pump beam waist radius is 80 μm. This plot shows the existence of different maxima. For a 0.43-cm-long crystal the maximum output power at 985 nm is obtained for an Yb concentration of 4.5×10^{19} ions/cm^3 (which is below the maximum possible Yb concentration of 6.8×10^{19} ions/cm^3 according to DeLoach *et al.*[21]). For a 0.8-cm-long crystal a similar maximum output power at 985 nm is obtained at an Yb concentration of 2.1×10^{19} ions/cm^3. In both case the unsaturated absorption of the pump in the crystal is approximately 80%.

To summarize, we have plotted optimized performance of the Yb:S-FAP laser in Fig. 12. Among the possible different crystal lengths that could optimize the output power we have chosen a 0.8-cm-long crystal to illustrate this optimization. This curve shows that our model predicts a cw output power of 460 mW for an incident pump power of 1.5 W and a double pass of the pump, as well as a slope efficiency of 39%. The optimized crystal depicted in Table 3 is approximately twice longer than our crystal, and its Yb concentration is slightly higher (2.1×10^{19} ions/cm^3 instead of 1.9×10^{19} ions/cm^3). The optimized beam sizes show that the beam waist has to be 1.6 times larger than the laser waist. The performance obtainable with this crystal is improved because of more efficient absorption of the pump.

5. DIODE PUMPING

As the ultimate aim of those interested in the Yb:S-FAP bulk crystal is to use diode pumping, we have to take into account the two major faults of powerful diode lasers, i.e., the wide spectrum and the poor quality of the beam. The laser diode considered for the numerical simulations here is one emitting 2 W at 899 nm with an emitting surface area of $1 \times 100\ \mu m^2$.

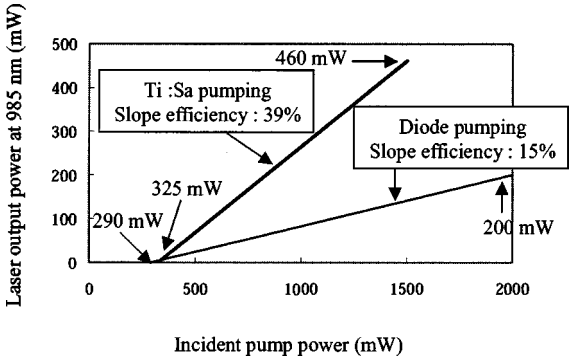


Fig. 12. Comparison of the optimized theoretical performance at 985 nm obtained with a Ti:sapphire pumping and a diode pumping in the double-pass configuration. The optimized Yb:S-FAP crystals are respectively described in Table 3 and Table 4. The diode used for the numerical simulations is a laser diode with a 1×100-μm^2 emitting area delivering a maximum output power of 2 W at 899 nm. The FWHM of the spectrum is 2 nm. In the direction parallel to the diode junction the beam quality factor M^2 is 15.

Table 3. Optimized Parameters of the Yb:S-FAP Crystal for Emission at 985 nm with Double-Pass Ti:sapphire Pumping[a]

Laser Beam Waist Radius	Output Coupler	Length	Yb Concentration
50 μm	8%	0.8 cm	2.1×10^{19} ions/cm^3

[a] Pump beam waist radius 80 μm.

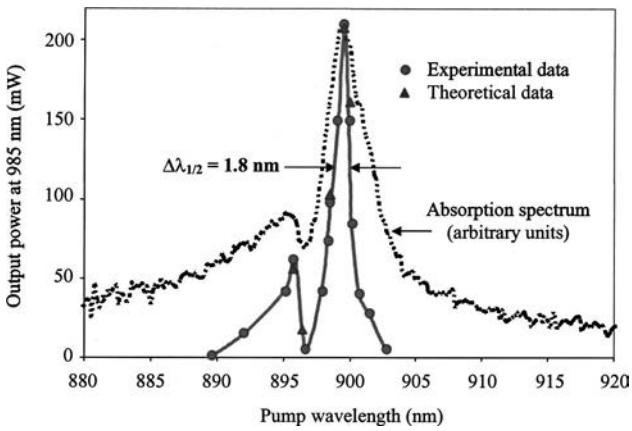


Fig. 13. Solid curve represents the output power at 985 nm versus wavelength of the Ti:sapphire pump for an incident pump power of 1.45 W. Circles, experimental data; triangles, theoretical data. Comparison is shown with the absorption spectrum (dashed curve).

First we have experimentally evaluated the pump spectral bandwidth that can lead to laser oscillation at 985 nm. In Fig. 13 we have plotted output power at 985 nm versus wavelength of a Ti:sapphire pump laser λ_p for an incident pump power of 1.45 W. Laser oscillation occurs from $\lambda_p = 889.5$ nm to $\lambda_p = 902.7$ nm and the FWHM of the main peak is approximately 1.8 nm, in the same range as the spectrum of laser diodes emitting 2 W with an emitting surface area of $1 \times 100\,\mu m^2$. We have also reported the values obtained from our model by varying the absorption cross section versus pump wavelength according to the Yb:S-FAP absorption spectrum given in Ref. 18. The experimental data are in good agreement with theory, showing that our model is realistic.

Second we have adapted our numerical model to pumping by a laser diode emitting a maximum cw output power of 2 W from a surface area of $1 \times 100\,\mu m^2$ in a poor-spatial-quality beam. In this condition there is no symmetry of revolution for the pump beam. We have introduced a beam quality factor M^2 of 15 in the direction parallel to the junction of the diode (termed x direction), whereas in the other direction (termed y direction) the beam is assumed to be diffraction limited.

The radius of the pump beam at the abscissa z in the crystal at $1/e^2$ of the maximum intensity along the x direction is

$$\omega_{p_x}(z) = \omega_{p_{0x}}\left\{1 + \left[M^2\frac{\lambda_p}{\pi n\,\omega_{p_{0x}}{}^2}(z - z_{p_{0x}})\right]^2\right\}^{1/2}. \quad (21)$$

n is the index of refraction of the crystal, $\omega_{p_{0x}}$ is the waist of the pump beam inside the crystal in the x direction, and $z_{p_{0x}}$ is its abscissa. In the following, we have considered that $z_{p_{0x}} = \ell/2$.

The radius of the pump beam at the abscissa z in the crystal at $1/e^2$ of the maximum intensity along the y direction is

$$\omega_{p_y}(z) = \omega_{p_{0y}}\left\{1 + \left[\frac{\lambda_p}{\pi n\,\omega_{p_{0y}}{}^2}(z - z_{p_{0y}})\right]^2\right\}^{1/2}. \quad (22)$$

$\omega_{p_{0y}}$ is the waist of the pump beam inside the crystal in the y direction, and $z_{p_{0y}}$ is its abscissa. In the following, we have considered that $z_{p_{0y}} = \ell/2$. The pump intensity is

$$I_p(x, y, z) = I_{p_0}(z)\exp\left[-\frac{2x^2}{\omega_{p_x}^2(z)}\right]\exp\left[-\frac{2y^2}{\omega_{p_y}^2(z)}\right]. \quad (23)$$

As in Section 2 we define and calculate the gain G per double pass:

$$G = \left\{1 + \int_0^\ell dz \int_0^{x_c}\int_0^{y_c}\frac{2g(x, y, z)}{\pi\omega_c{}^2(z)} \times \exp\left[-\frac{2(x^2 + y^2)}{\omega_c{}^2(z)}\right]dx\,dy\right\}^2, \quad (24)$$

with $x_c = y_c = r_c$.

Taking into account the wide spectrum of the diode and considering the good agreement between the model and the previous experiment (see Fig. 13), we have introduced an averaged absorption cross section $\sigma_{ap,m}$ at pump wavelength of

$$\sigma_{ap,m} = \frac{\sum_i \lambda_{p,i}\sigma_{ap,i}}{\sum_i \lambda_{p,i}}. \quad (25)$$

$\sigma_{ap,i}$ is the absorption cross section at the pump wavelength $\lambda_{p,i}$. We have considered that the spectrum of the diode is centered at 899 nm with a FWHM of 2 nm. Then we found $\sigma_{ap,m} = 4.9 \times 10^{-20}\,cm^2$.

Table 4. Optimized Parameters of the Yb:S-FAP Crystal for Laser Emission at 985 nm with Double-Pass Laser Diode Pumping

Pump Beam Waist Radius[a]	Pump Beam Waist Radius[b]	Laser Beam Waist Radius	Output Coupler	Length	Yb Concentration
60 μm	40 μm	40 μm	5%	0.6 cm	6×10^{19} ions/cm^3

[a] $\parallel$ to the diode junction
[b] $\perp$ to the diode junction

The best performance was predicted by our model with the crystal depicted in Table 4. This optimized crystal is slightly longer than our crystal (0.6 cm instead of 0.43 cm) and its Yb concentration is approximately three times higher. As for Ti:sapphire pumping, the pump beam waist is larger than the laser waist. As shown in Fig. 12 we were expecting a maximum output power of 200 mW at 985 nm with an incident pump power of 2 W in a pump recycling configuration. The laser threshold was calculated to be reached for an incident pump power of 290 mW, leading to a slope efficiency of 15%.

This study is the first step toward efficient diode pumping of an Yb:S-FAP bulk crystal for laser emission at 985 nm. Moreover, as the model can also be applied to other Yb-doped crystals we have numerically tested an Yb:KGW crystal, which is the second ranking crystal for pump intensity necessary to reach transparency (see Table 2). Even if the laser threshold is predicted to be higher (approximately 1.2 W when pumped at 935 nm with a laser diode having an emitting surface of $1 \times 100\ \mu m^2$ and using the same parameters as in Table 4) this crystal would be interesting to use since cw, commercial, powerful laser diodes at 935 nm and commercial Yb:KGW crystals would be easily available.

6. CONCLUSIONS AND PERSPECTIVES

To conclude, we have developed a numerical model specific to a cw Yb-doped bulk crystal laser emitting on a three-level transition near 980 nm. This model takes into account the saturation of absorption that is an important point in three-level lasers, as well as the spatial evolution of the pump and cavity beams. Our model has been validated by an experiment that resulted in a cw output power of 250 mW at 985 nm with an Yb:S-FAP crystal. This model has enabled us to establish the parameters that could optimize the performance of this three-level laser, such as the relative sizes of the beams inside the crystal, the optimal output coupler, the length of the crystal, and its doping. The main prospect is to diode pump the Yb:S-FAP crystal at 899 nm. As a result of running a preliminary experiment to simulate the wide spectrum of a laser diode and adapting our numerical model to the diode pumping, we are convinced that efficient diode pumping of an Yb:S-FAP crystal is possible. Moreover, our numerical model has shown that other crystals such as Yb:KGW would be interesting to use with a diode pumping at 935 nm.

ACKNOWLEDGMENTS

We acknowledge A. Bayramian and K. Shaffers from the Lawrence Livermore National Laboratory for the Yb:S-FAP crystal, the Laboratoire de Chimie Appliquée de l'Etat Solide de l'Ecole Nationale Supérieure de Chimie de Paris for the loan of their Ti:sapphire laser, and the NetTest company for the financial support of S. Yiou's PhD.

S. Yiou may be reached by telephone at 01 69 35 87 92, by fax at 01 69 35 87 00, and by e-mail at Sylvie.Yiou@iota.u-psud.fr.

REFERENCES

1. T. Maiman, "Stimulated optical radiation in ruby," Nature **4736**, 493–494 (1960).
2. C. Randy Giles and E. Desurvire, "Modeling erbium-doped fiber amplifiers," J. Lightwave Technol. **9**, 271–283 (1991).
3. C. Barnard, P. Mylinski, J. Chrostowski, and M. Kavehrad, "Analytical model for rare-earth-doped fiber amplifiers and lasers," IEEE J. Quantum Electron. **30**, 1817–1830 (1994).
4. L. D. Merkle, A. Pinto, H. R. Verdun, and B. McIntosh, "Laser action from Mn^{5+} in $Ba_3(VO_4)_2$," Appl. Phys. Lett. **61**, 2386–2388 (1992).
5. J. G. Lynn, R. C. Stoneman, and L. Esterowitz, "Three-level lasers end-pumped with laser diode bars," in *Advanced Solid-State Lasers*, G. Dubé and L. Chase, eds., Vol. 10 of OSA Proceedings Series (Optical Society of America, Washington, D.C., 1991), pp. 286–290.
6. J. D. Minelly, L. A. Zenteno, M. J. Dejneka, W. J. Miller, D. V. Kuksenkov, M. K. Davis, S. G. Crigler, and M. E. Bardo, "High-power, diode-pumped, single-transverse-mode, Yb Fiber Laser Operating at 978 nm," in *Optical Fiber Communications Conference*, Postconference Digest, Vol. 37 of OSA Trends in Optics and Photonics Series (Optical Society of America, Washington, D.C., 2000), postdeadline paper PD2.
7. K. H. Ylä-Jarkko, R. Selvas, D. B. S. Soh, J. K. Sahu, C. A. Codemard, J. Nilsson, S. A. Alam, and A. B. Grudinin, "A 3.5-W, 977-nm, cladding-pumped, jacketed-air-clad, ytterbium-doped fiber laser," in *Advanced Solid-State Lasers*, J. Zayhowski, ed., Vol. 83 of OSA Trends in Optics and Photonics Series (Optical Society of America, Washington, D.C., 2003), postdeadline paper PD2-1, p. 103.
8. K. Shaffers, J. Tassano, P. Waide, S. Payne, and J. Morris, "Progress in the growth of Yb:S-FAP laser crystals," J. Cryst. Growth **225**, 449–453 (2001).
9. A. J. Bayramian, C. Bibeau, R. J. Beach, C. D. Marshall, S. A. Payne, and W. F. Krupke, "Three-level Q-switched laser operation of ytterbium-doped $Sr_5(PO_4)_3F$ at 985 nm," Opt. Lett. **25**, 622–624 (2000).
10. S. A. Payne, L. D. DeLoach, L. K. Smith, W. L. Kway, J. B. Tassano, W. F. Krupke, B. H. T. Chai, and G. Loutts, "Ytterbium-doped apatite-structure crystals: a new class of laser materials," J. Appl. Phys. **76**, 497–503 (1994).
11. J. Armitage, "Three-level fiber laser amplifier: a theoretical model," Appl. Opt. **27**, 4831–4836 (1988).
12. J. Nilsson, J. D. Minelly, R. Paschotta, A. C. Tropper, and D. C. Hanna, "Ring-doped, cladding-pumped, single-mode, three-level fiber laser," Opt. Lett. **23**, 355–357 (1998).
13. W. P. Risk, "Modeling of longitudinally pumped solid-state lasers exhibiting reabsorption losses," J. Opt. Soc. Am. B **5**, 1412–1423 (1988).
14. T. Y. Fan and R. L. Byer, "Modeling and cw operation of a quasi-three-level 946 nm Nd:YAG laser," IEEE J. Quantum Electron. **23**, 605–611 (1987).
15. G. L. Bourdet, "Theoretical investigation of quasi-three-level, longitudinally pumped, continuous-wave lasers," Appl. Opt. **39**, 966–971 (2000).
16. C. Lim and Y. Izawa, "Modeling of end-pumped, cw, quasi-three-level lasers," IEEE J. Quantum Electron. **38**, 306–311 (2002).
17. F. Augé, F. Druon, F. Balembois, P. Georges, A. Brun, F. Mougel, G. Aka, and D. Vivien, "Theoretical and experimental investigations of a diode-pumped, quasi-three-level laser: the Yb^{3+}-doped $Ca_4(GdO(BO_3)_3$ (Yb:GdCOB) laser," IEEE J. Quantum Electron. **36**, 598–606 (2000).
18. L. D. DeLoach, S. A. Payne, L. K. Smith, W. L. Kway, and W. F. Krupke, "Laser and spectroscopic properties of $Sr_5(PO_4)_3F$:Yb," J. Opt. Soc. Am. B **11**, 269–275 (1994).
19. O. Svelto, *Principles of Lasers*, 4th ed. (Plenum, New York, 1998), pp. 60–62.
20. W. W. Rigrod, "Gain saturation and output power of optical masers," J. Appl. Phys. **34**, 2602–2609 (1963).
21. L. D. DeLoach, S. A. Payne, L. L. Chase, L. K. Smith, W. L. Kway, and W. F. Krupke, "Evaluation of absorption and

emission properties of Yb^{3+}-doped crystals for laser applications," IEEE J. Quantum Electron. **29**, 1179–1190 (1993).
22. D. S. Sumida and T. Y. Fan, "Effect of radiation trapping on fluorescence lifetime and emission cross section measurements in solid-state laser media," Opt. Lett. **19**, 1343–1345 (1994).
23. N. V. Kuleshov, A. A. Podlipensky, and V. P. Mikhailov, "Pulsed laser operation of Yb-doped $KY(WO_4)_2$ and $KGd(WO_4)_2$," Opt. Lett. **22**, 1317–1319 (1997).
24. T. Y. Fan and A. Sanchez, "Pump source requirements for end-pumped lasers," IEEE J. Quantum Electron. **26**, 311–316 (1990).